Photonic Beamformer Model Based on Analog Fiber-Optic Links' Components

V A Volkov[1], D A Gordeev[1], S I Ivanov[2], A P Lavrov[2], I I Saenko[2]

[1] Open Joint Stock Company "Research Institute "Vektor", Academician Pavlov str. 14a, Saint Petersburg 197376, Russia
[2] Peter the Great St.Petersburg Polytechnic University, Polytechnicheskaya str. 29, Saint Petersburg 195251, Russia

e-mail: lavrov@ice.spbstu.ru

Abstract. The model of photonic beamformer for wideband microwave phased array antenna is investigated. The main features of the photonic beamformer model based on true-time-delay technique, DWDM technology and fiber chromatic dispersion are briefly analyzed. The performance characteristics of the key components of photonic beamformer for phased array antenna in the receive mode are examined. The beamformer model composed of the components available on the market of fiber-optic analog communication links is designed and tentatively investigated. Experimental demonstration of the designed model beamforming features includes actual measurement of 5-element microwave linear array antenna far-field patterns in 6-16 GHz frequency range for antenna pattern steering up to 40°. The results of experimental testing show good accordance with the calculation estimates.

1. Introduction

Operation in an ultrawide frequency band (over several octaves) is highly desirable for some up-to-date types of phased array antennas (PAA). Beamformers based on true-time-delay (TTD) technique permit to form scanning PAA beam or a set of switched beams free of squint effect and achieve ultrawideband array antennas operation. For the last decades, the TTD beamforming has been often associated with photonic technologies, in view of their advantages compared with traditional electronic technique, such as wide instantaneous bandwidth, low loss in signal transmitting, small size and weight, high resistance to electromagnetic interference and flexible designing [1 - 3]. So, applying the microwave photonic devices for development of PAA beamforming systems affords the means to overcome conventional radio electronic beamformer limitations. Therefore, many beamforming architectures based on microwave photonics have been proposed and evaluated in the past years, for PAA both in transmission and reception modes. Most of the proposed architectures using fiber optic components to provide control of one- or multibeam antenna array pattern require specially developed units, such as chirped fiber Bragg gratings, fast tunable lasers with narrow spectral linewidths, reflection fiber segments, optical filter arrays and others. Meanwhile, up to date some manufactures have developed a family of microwave photonic links operating up to 40 GHz, offering various levels of bandwidth, noise figure and dynamic range. The performance characteristics of these modern analog photonic data communication links' components have attained the level, which allows their using to construct experimental prototypes of PAA beamforming systems and further designing of advanced beam forming network. Implementation of widely developed analog fiber-optic link components to compose

the antenna array beamformer (BF) arrangement has been extensively investigated [4 - 6]. Some of proposed architectures were found to be the most suitable for this way of BF prototype designing; however, there are special requirements (namely, phase-frequency dependence, intrinsic time delays in transmitter and receiver modules) which the BF photonic components have to meet anyway while the fiber-optic communication links manufacturers do not take them into account. Here we consider TTD photonic BF for PAA in receive mode based on dense wavelength division multiplexing (DWDM) components and chromatic dispersion of a single mode optical fiber and implemented with units and components available at the market of modern fiber-optic communication systems [6]. Also we present some results of a kind of BF experimental model assembling and adjustment and its performance investigation including the microwave receiving linear PAA far-field pattern measurement in the 6-15 GHz frequency band. Experimental results show squint-free beamforming achieved with the proposed beamformer model.

2. Photonic Beamformer Model Architecture and Principle of Operation

The developed beamformer architecture based on the components implementing a DWDM technology approach and optical fiber chromatic dispersion is shown in Figure 1 [4, 6, 7]. This scheme is designed for the N element's linear PAA and uses optical comb – a set of N lasers with different but uniformly spaced (step $\Delta\lambda$) wavelengths, the total wavelength band is $(N - 1)\cdot\Delta\lambda$. The RF signals from the antenna elements A_1 .. A_N modulate a set of laser diodes. Electrooptic conversion is achieved either by

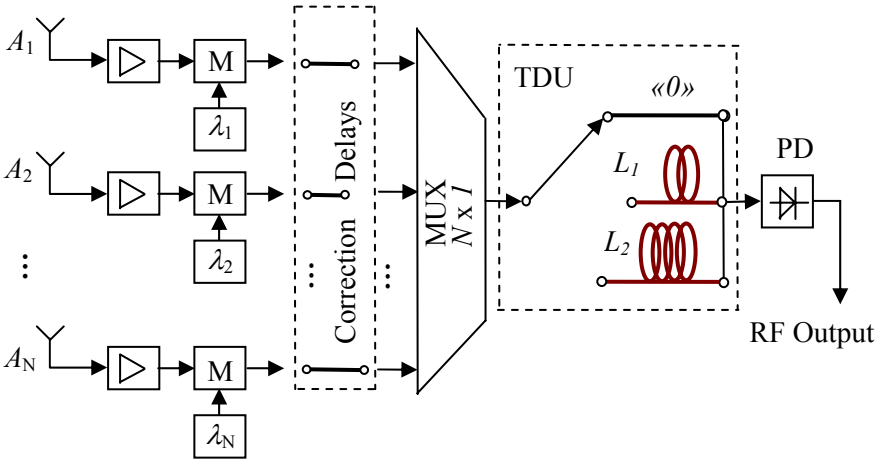

Figure 1. Architecture of photonic beamformer with fiber chromatic dispersion based interchannel delays.

direct modulation of a lasers or by using an external modulators as represented in Figure 1 (scheme elements M). Further, the intensity-modulated optical carriers are combined into a single fiber by a multiplexer (MUX N x 1 unit) and fed into a time delay unit (TDU). For practical application TDU may include one optical switch n x n and (n - 1) fiber segments whose lengths vary exponentially: ΔL, 2 ΔL, 4 ΔL, etc. as in [7]. Switch control allows to change the total length of the fibers from ΔL to $L = (2^{n-1} - 1)\,\Delta L$ with increment ΔL. As all the optical carriers share with the same light paths, the time delay differences between adjacent channels are produced by the fiber chromatic dispersion D measured in ps/(nm·km). Time delay $\tau = \Delta\lambda\cdot L\cdot D$ introduced between adjacent channels results in the respective tilting of PAA beam. Photodiode (PD) at TDU output converts sum of delayed intensity-modulated optical carriers back to microwave domain. In Figure 1 instead of optical switch n x n and (n - 1) fiber segments one can see 2 fiber lengths L_1 and L_2 successively inserted between the multiplexer and the photodiode thus giving (together with "*0*" - length position) 3 interchannel delay

values: 0, τ_1 and τ_2 corresponding to 0, θ_1 and θ_2 beam pointing angles. The "Correction Delays" unit contains fiber segments with strictly sized up lengths equalizing the interchannel delays from RF sources (scheme elements A_1 .. A_N) to the MUX output. Hence, it corresponds to a flat phase law tilted 0 to PAA base line – the PAA beam directed normal to PAA base.

In the considered architecture of 1-D beamformer the number of PAA beams can be increased (as for example in [4]) that only requires a higher splitting ratio and another set of dispersive fibers and photodiodes.

3. Research of Photonic Beamformer Key Components

Among the photonic BF model's key components depicted in Figure 1 the units converting radio signal into optical one (laser jointly with modulator) and backward (photo receiver) are crucial for BF correct performance. In our BF model arrangement the transmitters and receiver modules from analog fiber-optic links OTS-2-18 (Emcore [8]) were used which can operate at 0.1..18 GHz bandwidth. In-built microprocessor-based transmitter control for laser bias and temperature as well as Mach-Zehnder modulator bias provides better consistent performance operation and allows for appreciably reduce the measurement results variations. The receiver module has an additional RF amplifier with 15 dB gain after photodetector. Transmitter unit includes 3 separate optically combined elements: DFB laser with wavelength corresponding to ITU grid with 100 GHz step, $LiNbO_3$ Mach-Zander modulator (MZM) with half-wave voltage approx. 5.8 V, optical 10 dB directional coupler and photodiode for MZM quadrature working point stabilization. Transmitter optical power in the fiber is about 10 dBm.

Figure 2 shows the transfer function $P_{OUT}(P_{IN})$ for one of OTS-2-18 links. It was measured with two input RF signals with frequencies 3.99 and 4.00 GHz and equaled powers: the principal harmonic power (line 1), the third order intermodulation response (line 2), and the receiver output noise P_{min} = – 155 dBm, averaged through the total frequency bandwidth 18 GHz and related to the 1 Hz bandwidth. More detail performance characteristics estimations are given in [9].

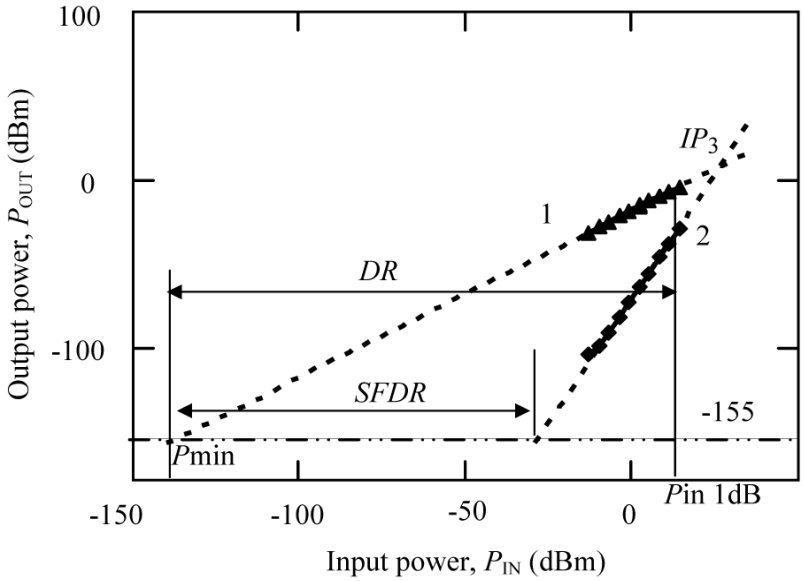

Figure 2. Fiber-optic OTS-2-18 link transfer function.

The noise power was measured with unmodulated receiver optical input (approx. 10 dBm). The measured link gain ranges from –3 dB at 1 GHz to –7 dB at 18 GHz. The 1 dB compression point $P_{IN\ 1dB}$ = 16.5 dBm, and the minimum input level is –144 dBm (when line 1 crosses the noise level P_{min}). Thus, the 1 dB compression dynamic range comes to 160.5 dB and the spurious free dynamic range is about 113 dB. The input signal level *IP*3 corresponding to the third order intermodulation products amounts to 25 dBm (P_{IN} when lines 1 and 2 are intersected).

The channels' phase-frequency characteristics are highly significant for BF performance. Figure 3 shows both of the total phase-frequency characteristic (argument of $S_{21}(f)$) and its deviation $\Delta\varphi(f)$ from a linear function for the frequency band of up to 20 GHz. It was measured for direct connection of transmitter and receiver units. One can see significant link time delay. Intrinsic time delays brought by link modules were measured separately and resulted in amount up to 17.4 ns for transmitter and 15.6 ns for receiver modules.

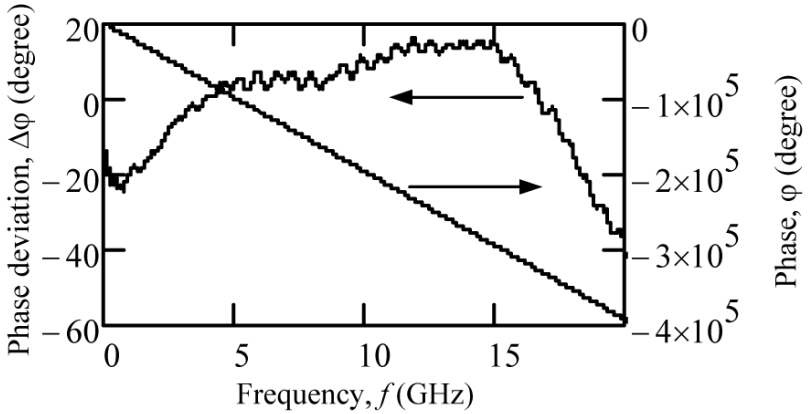

Figure 3. Phase-frequency response for OTS-2-18 link.

Summation of optical signal from transmitters is fulfilled by 8-channel multiplexer whose channels are centered in accordance with ITU standard channels from 27 to 34 with 100 GHz step. Its insertion loss is approx. 1.5 dB, –1 dB bandwidth approx. 65 GHz, that is sufficient for transmission of intensity modulated optical carrier with RF frequencies up to 20 GHz and more. Nevertheless, it should be mentioned that all of the transmitters' and corresponding multiplexer channels' midmost wavelengths have to be accurately alignment according to ITU channel plan and avoid mismatching during operation. We have measured passband characteristics for all multiplexer channels with optical spectrum analyzer and found good wavelengths setting and flat-shape channel passband curves behavior [10].

As it was pointed earlier one need to align the delays of all BF channels from MZM inputs to common MUX output. This can be done by insertion of equalizing fiber patch cord in each BF channel (see Figure 1: Correction Delays unit). We measured channels time delays τ_{CH} by Vector Network Analyzer (R&S, ZVA 40) using the relation: $\arg[S_{21\,k}(f)] = 2\pi f \cdot \tau_{CH}$. Further one can calculate necessary lengths of corrective patch cords for all BF channels to provide their identical delays at the TDU input. TDU in BF model consists of SM fibers with lengths labeled 0, L_1, L_2 corresponding to PAA beam pointing angles θ_0, θ_1, θ_2 in accordance with relation $L = d \cdot \sin(\theta)/(c \cdot D \cdot \Delta\lambda)$ where d is the distance between neighboring antenna elements and c is the speed of light in a vacuum.

4. Beamformer Model Design and Setup

Initially BF model was intended for measurements in conjunction with PAA with element spacing $d = 25$ mm. However actual measurements with 1-D PAA for demonstration of the designed BF model beam steering performance were accomplished with wideband 1-D PAA composed of $d = 10$ mm spaced Vivaldi patch radiating elements. To approximate the initially chosen range of delays between BF channels (and dispersion fiber lengths L_1, L_2) with the distance between radiating elements the last ones were connected to five BF inputs selectively through one thus giving radiating elements actual spacing $d = 20$ mm. This spacing jointly with specified BF dispersion fiber lengths $L_1 = 1600$ m, $L_2 = (L_1 + 1500)$ m and 0.8 nm wavelength spacing (100 GHz ITU grid) results in beam pointing angles $\theta_0 = 0°$, $\theta_1 = 18.9°$, $\theta_2 = 38.7°$. The dispersion fiber lengths were made as two coils of standard SMF-28 fiber with lengths 1600 m and 1500 m and chromatic dispersion about $D = 17$ ps/nm·km.

The results of time delay measurements of used components have been converted to their tantamount electrical lengths. Because of large difference in electrical length of our MUX channels

(up to 6 m, as 8 x 1 MUX from ATW has inner structure as a chain) we have replaced the MUX by 8 x 1 splitter/combiner ($LiNbO_3$ Planar Light Circuit, PLC). Optical losses in 8 x1 combiner channels were 11.5±0.35 dB, channels electrical lengths (relying on 1 m patch-cords) were in range 1558.1±1.2 mm. Hereafter five corrective patch-cords with the calculated lengths: 200, 226, 254, 550, 624 mm were made and inserted in BF model channels at the combiner inputs. Table 1 shows the results of time delays alignment in designed BF model (with corrective patch-cords) for 3 beam positions: $\theta_0 = 0^\circ$, $\theta_1 = 15^\circ$, $\theta_2 = 30^\circ$. 'Exp' means experimental value, 'Calc' means expected (calculated) value. PAA channel numbers (as to its central element) are +2, +1, 0, –1, –2 and they are connected with transmitter units OTS-2T with ITU channel numbers 27, 28, 29, 30, 31 respectively. Angles $\theta_0 = 0^\circ$, $\theta_1 = 15^\circ$, $\theta_2 = 30^\circ$ are given for case "initial" PAA with d = 25 мм.

Table 1. Time delays adjustment in BF model for 3 beam positions.

Channel # in PAA	ΔS_{21}, dB	$\Delta\tau_{CH}$, ps, Exp / Calc		
		$\theta_0 = 0^\circ$, $L_0 = 0$ m	$\theta_1 = 15^\circ$, $L_1 = 1600$ m	$\theta_2 = 30^\circ$, $L_2 = 3100$ m
+ 2	–1.4	0.05 / 0.0	43.03 / 43.14	83.48 / 83.33
+ 1	1.2	0.003 / 0.0	21.90 / 21.57	42.68 / 41.67
0	0.1	0.44 / 0.0	0.0	0.0
– 1	1.4	–1.89 / 0.0	–22.56 / –21.57	–43.12 / –41.67
– 2	–1.3	1.41 / 0.0	–42.64 /–43.14	–82.75 / –83.33

The values in columns 2 and 3 show results of BF model alignment in its initial state $\theta_0 = 0^\circ$, they are given relatively to mean values over five channels. S_{21} mean value was –25.0 dB, mean value of electrical length over 5 BF channels was 11.708 m. Time delays in columns 4 and 5 are given relatively to delays for central PAA element #0, serviced by the laser with a wavelength at ITU channel #29. These delays are measured at RF frequencies near 4 GHz. Because of small differences between 'Exp' and 'Calc' time delay values in columns 4, 5 one can expect BF model functioning in wide frequency range with no squint effect.

5. Photonic BF Model Test Results

An experimental demonstration of the BF prototype performance consisted in far-field pattern measurements of the 1-D antenna array assembled with the photonic BF model in anechoic chamber. In our pattern measurements a wideband reference horn fed by a vector network analyzer (with additional RF power amplifier) radiates a microwave signal. The PAA under test located in front of the reference horn is fixed on an azimuth scan drive. The distance between the horn and array is about 6 m to fulfill far-field condition requirement. Microwave signal from BF (RF output of its optical receiver unit) is returned to vector network analyzer and compared with signal that feeds through RF power amplifier reference horn during azimuth scan. For each azimuth position – 1º step – network analyzer scans wide frequency range from 6 to 15 GHz. These measurements have been done for 3 different lengths of dispersive fiber in our TDU.

Figure 4 represents the far-field patterns measured with the BF for 3 optical fiber lengths at the middle frequency 9 GHz. Insertion of 0, 1600 and 3100 m optical fibers shifts the antenna pattern to $\theta_0 = 1.3^\circ$ (red), $\theta_1 = 18.8^\circ$ (blue), and $\theta_2 = 36.8^\circ$ (green), respectively. The measured shifts are close to the calculated ones when time delays between two neighbouring radiating elements are 0, 21.57, 43.14 ps, see Table 1. Small "0"- beam deviation from the normal position (0º) was generated by residual differences about a few tenth of a millimeter in total channel electrical lengths including RF cables between PAA and the BF model inputs. The sidelobe level for $\theta_0 = 1.3^\circ$ is approx. –13 dB in accordance with the uniform amplitude distribution. Figure 5 shows the far-field patterns in polar form for 3 optical fiber lengths at frequencies 6 (red), 9 (blue), and 12 GHz (green), respectively. One can see no squint effect in wide frequency range for PAA with designed photonic BF model.

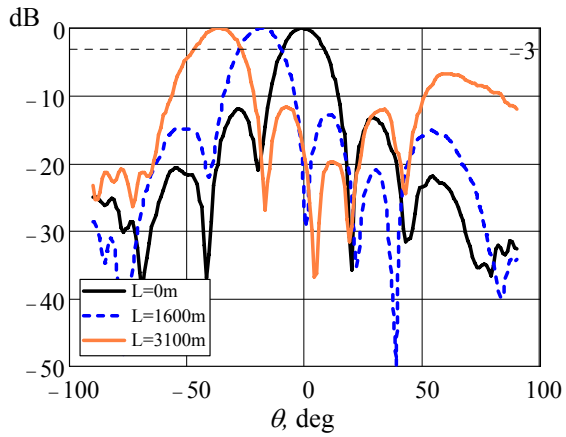

Figure 4. The PAA far-field patterns at 9 GHz: control of beam position.

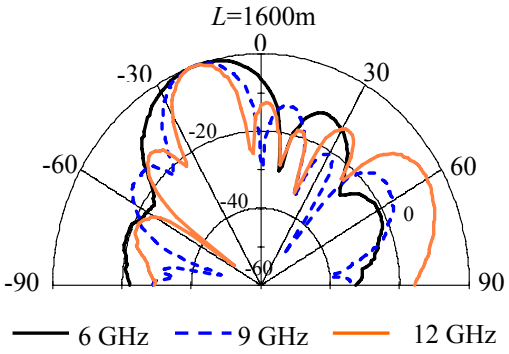

Figure 5. The PAA far-field patterns for 6, 9, and 12 GHz at 18.8º, no squint effect.

6. Conclusion

The model of photonic beamformer for ultrawideband microwave phased antenna array has been developed and tested. We have demonstrated the ability of 1-D BF based on DWDM multiplexing and optical fiber chromatic dispersion to steer the beam of PAA in the receive mode. This BF architecture realizes true-time-delay approach to beam steering where different time-delay distributions are provided with a set of dispersive fiber lengths. The beamformer model containes the components available on the market of fiber-optic analog communication links. Experimental demonstration of the designed model beamforming features includes actual measurement of 5-element microwave linear array antenna far-field patterns for 3 beam directions up to 36º at frequencies 6..12 GHz. The results of BF model experimental testing show no squint effect and good accordance with the calculation results.

References

[1] 2009 *Microwave Photonics: Devices And Applications ed S Iezekiel* (Chippenham: Wiley-IEEE Press)
[2] Tur M, Yaron L, Rotman R and Raz O 2011 *Proc. OSA/OFC/NFOEC 2011 (Los Angeles)* Paper OThA6
[3] Yao J P 2012 *IEEE Photonics Society Newsletter* **26**(3) 5-12
[4] Blanc S, Alouini M, Garenaux R, Queguiner M and Merlet T 2006 *IEEE MTT Trans.* **54** 402-11
[5] Minasian R A, Chan E H W and Yi X 2013 *Optics Express* **22**(19) 22918-36
[6] Lavrov A P, Ivanov S I and Saenko I I 2014 *Internet of Things, Smart Spaces, and Next Generation Networks and Systems ed S Balandin et al* ser. *LNCS* 8638 (Springer Int. Publ. Switzerland) pp 647-55
[7] Yang Y, Dong Y, Liu D, He H, Jin Y and Hu W 2009 *Chinese Optics Lett.* **7** 118-20
[8] http://emcore.com/wp-content/uploads/2016/03/Optiva-OTS-2-18GHz-Unamplified.pdf
[9] Ivanov S I, Lavrov A P and Saenko I I 2015 *J. Opt. Technol.* **82**(3) 139-46
[10] Ivanov S I, Lavrov A P and Saenko I I 2015 *Proc. 2015 Int. Siberian Conf. on Control and Communications (SIBCON) (Omsk, Russia)* (New York: IEEE) pp 1-4